Intrinsic Amorphous Silicon Bilayers for Surface Passivation in Silicon Heterojunction Solar Cells

Busra Altinsoy*[1,2], Valerie Depauw[3,4,5], Devika Rajagopal[3,4,5,6], Hariharsudan Sivaramakrishnan Radhakrishnan[3,4,5], Hisham Nasser[1], Rasit Turan[1,2,7]

[1]ODTÜ-GÜNAM, Middle East Technical University, 06800 Ankara, Türkiye
[2]Micro and Nanotechnology Graduate Program of Natural and Applied Sciences, Middle East Technical University (METU), 06800 Ankara, Türkiye
[3]Imec, imo-imomec, Genk, 8320, Belgium
[4]Energyville, imo-imomec, Genk, 8320, Belgium
[5]University of Hasselt, imo-imomec, 3590, Belgium
[6]KU Leuven,3001, Belgium
[7]Department of Physics, Middle East Technical University (METU), 06800 Ankara, Türkiye

*Corresponding author. E-mail address: busraaltinsoy@gmail.com

Abstract

The performance of Silicon Heterojunction Solar Cells is tied to specific properties of hydrogenated amorphous silicon (a-Si:H) thin layers particularly as passivating contacts. This study provides insights into the structure and thickness optimization of intrinsic amorphous silicon (i-aSi:H) bilayers obtained by combining two layers deposited under different process conditions to enhance passivation quality. Through systematic variation of deposition parameters, the optical properties and Si-H bonding configuration of the resulting thin films are characterized using ellipsometry and ATR spectroscopy, respectively. Microstructure factors are derived to interpret the porosity of the layers based on ATR results. Bilayers with a total thickness of 10 nm consisting of a porous interfacial layer and a dense overlying layer are applied on c-Si surface. The optimum thickness(~3nm) and microstructure factor (~0.5) for the first layer are investigated to increase the passivation at the c-Si and i-aSi:H interface. Furthermore, the impact of post-hydrogen plasma treatment (HPT) time on minority carrier lifetime is investigated. The results show that increasing the post-hydrogen plasma treatment time has a more significant effect when the porous layer is thinner.

Keywords:
Surface passivation
Amorphous Silicon Bilayers
PECVD
Silicon heterojunctions
Solar cells

1.Introduction

The Silicon Heterojunction (SHJ) solar cell technology emerges as a leading choice, highlighting an exceptional history of efficiency. It holds the current efficiency record of 26.81% for single-junction solar cells based on crystalline silicon (c-Si)[1]. High V_{oc} values observed in SHJ solar cells are largely attributed to hydrogenated intrinsic amorphous silicon (i-a-Si:H) layers providing high-quality chemical passivation of the c-Si surface. Passivation at c-Si and i-a-Si:H interface was explained by hydrogen diffusion, hydrogenation of silicon dangling bonds and reduction of interfacial defect density[2]. Optimization of deposition conditions of the intrinsic hydrogenated amorphous silicon (i-a-Si:H) layer, understanding of their properties, and role on the solar cell performance are essential to enable high-efficiency solar cells. While porous intrinsic a-Si:H films with high void and defect density may not be effective in terminating dangling bonds on the c-Si surface, dense i-aSi:H films deposited by hydrogen-diluted plasma are beneficial to the solar cell parameters but the formation of epitaxial crystallization of silicon[3] and defects such as twins or stacking faults might occur. Qu, X. et al uncovered that nanotwins generated during intrinsic amorphous silicon depositions leads grain boundaries by high annealing temperature and they generate deep levels in the band gaps[4]. Bilayers balance a porous interfacial layer preventing epitaxial growth with an additional dense layer to achieve better passivation at c-Si and i-a-Si:H interface[5].

In this work, we deposited i-a-Si:H layers by parallel plate radio frequency Plasma Enhanced Chemical Vapor Deposition (rf PECVD) and report the optical and hydrogen bonding characteristics of them. Bilayers (i1/i2) are applied on both sides of n-type low resistivity textured c-Si wafers, and we try to propose optimum deposition and hydrogenation parameters to improve minority-carrier lifetime and understand how their properties correlate with it. Pure SiH_4 plasma, expected to lead to a porous layer, is usually used for the growth of a first intrinsic layer[6–8]. We introduced hydrogen-diluted plasma (SiH_4:H_2 = 1:4, 1:3 or 1:2) during depositions of both intrinsic a-Si:H layers because Meddeb et al. observed that epitaxial growth was also avoided for films deposited at a plasma power of 100 W, when the hydrogen dilution ratio is less than 5 (SiH_4:H_2 = 1:5)[9]. Because the faster deposition leads to disordered a-Si:H films, a high deposition rate can also suppress epitaxial growth in the initial stage. We introduced higher deposition powers for i-a-Si:H (i_1) buffer layer to leverage this inhibition.
The passivation quality of bilayers (i_1/i_2) is checked by focusing on the porosity and thickness of first intrinsic layer (i_1) on the c-Si surface. The effect of hydrogen plasma treatment (HPT) time on the minority carrier lifetime is also investigated.

2. Experimental Details

The wafers were cleaned using imec's industrial cleaning process involving deionized water, hydrofluoric acid and ozone (DIW: HF: O_3). Prior to the depositions, an HF dip is done to ensure the removal of native silicon oxide. Fast transfer to the PECVD system is necessary to avoid reoxidation. PECVD in a parallel plate radio frequency at 13.56 MHz AK1000 Inline system from Roth & Rau was used for the i-a-Si:H film preparation. The substrate temperature T and pressure p were set to T = 175 °C, p = 2.3 mbar, respectively. The silane flow rate was $QSiH_4$ = 160 sccm, and the plasma was diluted with H_2 flow.
Series of intrinsic a-Si:H layers were deposited using different plasma powers on one-side mirror polished Cz-Si wafers (725 µm thick) for ellipsometry characterization. Thickness of layers was controlled by varying the deposition times. The thickness, band gap (based on Tauc-Lorentz) and the refractive index of layers were determined by spectroscopic ellipsometry. Deposition rates were calculated using thickness obtained from ellipsometry analysis. However, to report the thickness on

textured wafers, we took measurements from the polished wafers placed alongside them during depositions. All the thickness values provided in this paper are for the layers on polished wafers. When the same process parameters are used, the actual thickness of each layer on textured wafers is expected to be thinner.

25 nm i-a-Si:H films were deposited on one-side mirror polished Cz-Si wafers (725 µm thick) for FTIR characterization. First, ATR measurements were initially taken from bare silicon (Si), followed by measurements from silicon with an amorphous coating. By subtracting the spectrum of the bare silicon from that of the coated silicon, the resulting spectrum isolated only the peak corresponding to the amorphous coating.

We applied intrinsic bilayers on both sides of P-doped, ~2 Ωcm, 170 µm, <100> oriented, textured (random pyramids with KOH etching) c-Si wafer. The first i-layer (i1) is grown with plasma diluted at different flow ratios (SiH_4:H_2) and at high process powers (>= 200 W), while the second i-layer (i2) is grown with hydrogen diluted plasma (SiH_4:H_2=1:4) at 50 W.

Quasi-steady state photoconductance (QSSPC) measurements were performed on these wafers to characterize the effective lifetime, and by extension the passivation quality. Photoluminescence imaging (PL) was used to assess the uniformity of the passivation. The QSSPC and PL measurements were carried out using BT imaging's proprietary PL imaging tool. Prior to each coating process, a trial run was conducted under standard operating conditions and lifetime was measured to check the status of the PECVD tool.

3. Results and Discussions

3.1 Impact of Power Density on Porosity of Intrinsic Layers

First, plasma power for growing i-aSi:H layers with different porosities were swept. Optical properties are characterized by spectroscopic ellipsometry. The deposition rate increases monotonically from 0.18 nms^{-1} to 1 nms^{-1} with increasing Pd from 20 mW cm^{-2} to 120 mW cm^{-2} (Figure 2a). However, when process power further increased to 160 W cm^{-2}, it only increased 10 %. For such high powers, H+ bombardment is increasing, and ion etching occurs. As a result, the competition between layer growth and etching becomes apparent.

The hydrogen bond configuration at the interface of a-Si:H and c-Si has been investigated by Fourier transform infrared spectroscopy. Changes in porosity of amorphous layers by the formation of vacancies and voids can be interpreted by the microstructure factor (R*) related to Si-H and Si-H_2 bonds[10,11]. R* is calculated from Si–H stretching mode signals in FTIR spectra (Figure 2) by fitting with Gaussian functions for deconvolution of absorption intensities of high ($\mathbf{I}_{HSM}$) and low ($\mathbf{I}_{LSM}$) stretching bonds (Figure 7).

The microstructure factor (R*) is calculated as:

$$\mathbf{R^*} = \mathbf{I}_{HSM} / (\mathbf{I}_{LSM} + \mathbf{I}_{HSM})$$

H content of layers can be calculated from the analysis of microstructure parameter; it is related to peak intensities of low and high stretching modes, are centered around 2000 cm^{-1} and 2100 cm^{-1}, respectively. Since poly-silanes (SiH_2 or SiH_3) on a void surface contribute significantly to the high stretching mode vibrations, its proportionality constant influencing total hydrogen content is higher than absorption of low stretching mode associated with compact hydrogen vibrations (Si-H)[12]. A higher R* value indicates a greater density of nano-sized voids within the a-Si films.

Fig. 1. Relationship between porosity and total hydrogen content in i-a-Si:H thin films.

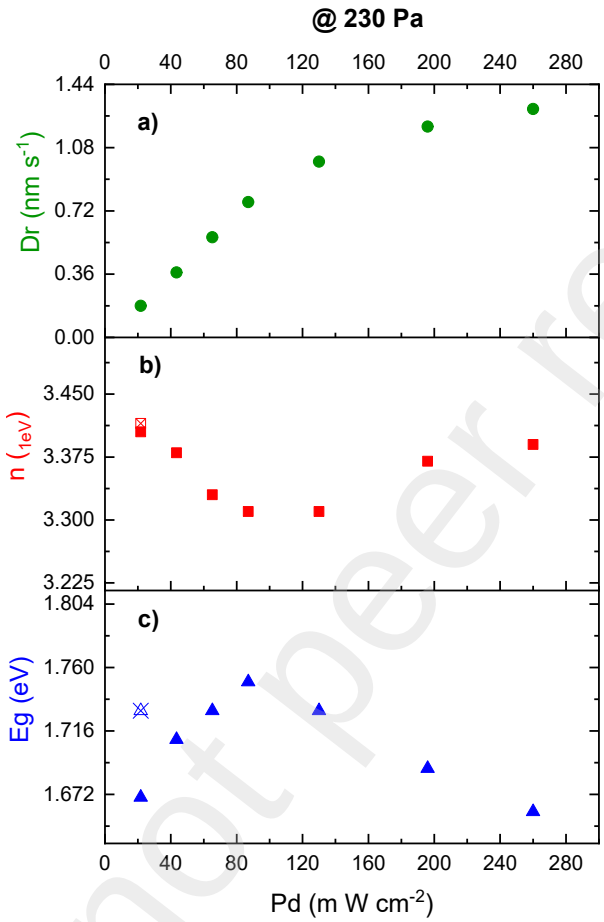

Fig. 2. a) Deposition rate, b) refractive index (n_{1eV}) and (c) optical bandgap (Eg, Tauc gap), of thin a-Si:H films (10 nm) as functions of the power density in PECVD process. Band gap and n_{1eV} are also measured for the films deposited at 20 mW cm^{-2} after post HPT process.

Peak shift is observed for the absorption of high-stretching modes to lower wavenumber with an increase in the peak intensity when power density increased from 20 mWcm^{-2} to 80 mW cm^{-2} then turns to shift oppositely with a decrease in the intensity when power density further increased to 120 mW cm^{-2} (Figure 3). R* increases from 0.16 to 0.69 with increasing power density up to 80 mW cm^{-2}. It can be interpreted that porosity and total hydrogen content of the layers increased according to micro-structure factor(R*) obtained from FTIR spectra. Increase in band gap ascribed to hydrogen content[6] also observed (Figure 2c). As observed from the deposition rates, etching intensifies with stronger H+ bombardment and denser layers (n_{1eV} is increasing) with lower hydrogen content (Eg is decreasing) grow (Figure 2). As a result, R* decreases from 0.63 to 0.43 when Pd increases from 80 mW cm^{-2} to 160 mW cm^{-2} (Figure 3). We would like to note that the power density values are calculated from the process power to determine the amount of power per unit area. For example, a 300 W process power corresponds to a 120 mW cm^{-2} power density.

Eventually, although we used hydrogen-diluted plasma, some of these R* values (Figure 3) are comparable to other measurements for under-dense layers grown with pure silane[5,7,13]. FTIR

characterization was conducted using 25 nm i-a:Si:H layers to determine the R* value. Notably, even higher R* values could potentially be observed with thinner films, as the R* value exhibits a strong dependence on thickness, particularly in the ultra-thin regime[14].

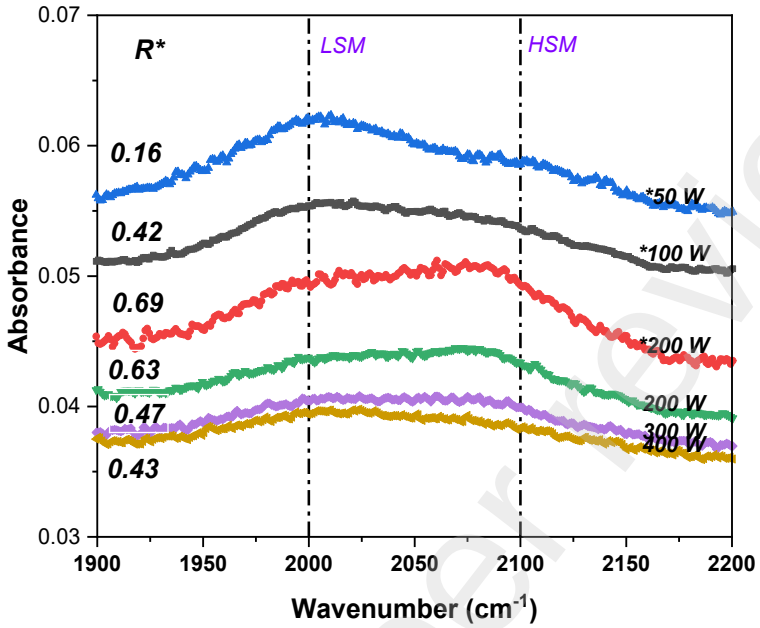

Fig. 3. Microstructure factor (R*) and absorbance spectra of the 25 nm a-Si:H films grown with SiH_4:H_2 1:4 plasma.
*The process powers are reduced to the actual deposition power after the plasma was ignited at 300 W for 1 second to be able to process at low process power.

Figure 4 shows the corresponding band gap of the thin films of various thicknesses. Band gap of the ultra-thin film deposited at any process power is higher than that of thicker films, indicating an increase in the amount of hydrogen. It has been reported that the void volume fraction in a-Si:H might be higher within a few nanometers of the a-Si:H/c-Si interface than bulk[15]. High number of poly-hydrides in the voids can extend the band gap of the i:a-Si:H.

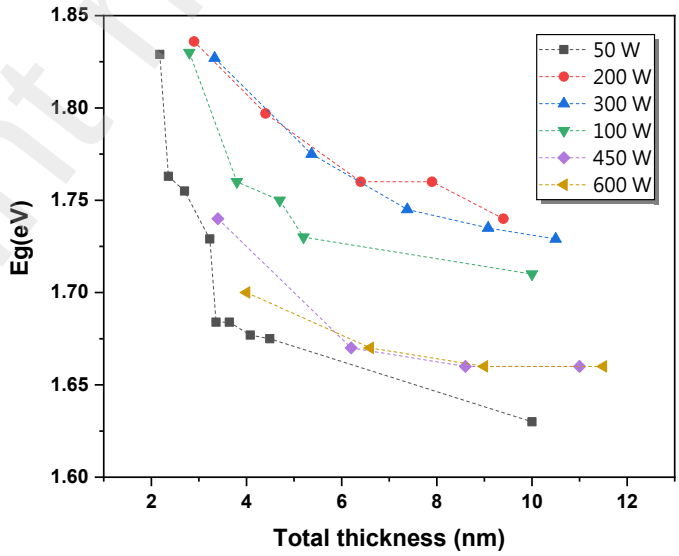

Fig. 4. Band gap of thin films grown at different power densities as a function of thickness.

3.2 Impact of First Layer Thickness on Carrier Lifetimes

In the second stage, we investigated the effect of the thickness of the i_1 layer with a large R* on minority-carrier lifetime at the a-Si:H/c-Si interface on a symmetric structure (Figure 5). Process power for i2 layer deposition was 50 W. Also post hydrogen treatment was applied at 50 W for 34 second after bilayer depositions. The i_1 layer thickness was varied from 1.1 to 9.9 nm and total thickness is kept at ~10 nm. The optimum surface passivation (2 ms) was obtained using a 2.2 – 4.4 nm i_1 porous layer. When 1.1 nm of the porous layer deposited at 300 W was used, the lifetime was lower (1.3 ms) because of the incomplete coalescence of the initial nuclei [16]. However, after 2.2 nm, the porous layer completely covered the surface, and the minority carrier lifetime increased. Because the amount of hydrogen in the nucleation layer (~ 2-3 nm), where epitaxial growth also can be observed, is further increased by using 300 W deposition power instead of 50 W for early stage of the growth. Band gap is higher when a 4 nm film is deposited at 300 W instead of 50 W as can be seen in Figure 4. Lifetime started to decrease when i_1 layer thickness became 6.6 nm. While the continuation of the porous layer at the interface through the nucleation layer increases passivation, using a porous layer thicker than 4 nm at the interface is more unsuitable for the hydrogen passivation. The single 10 nm of porous i_1-layer resulted in the lowest lifetime (Figure 5). The porous layer was only beneficial for the nucleation part of the intrinsic aSi:H film. We assume this could be attributed to the defective nature of the porous layer rich in terms of Si-H_2 bonds. H atoms in the form of Si-H bonds were preferred than those in the form of Si-$H_{2,3}$ bonds for better passivation [17,18][19].

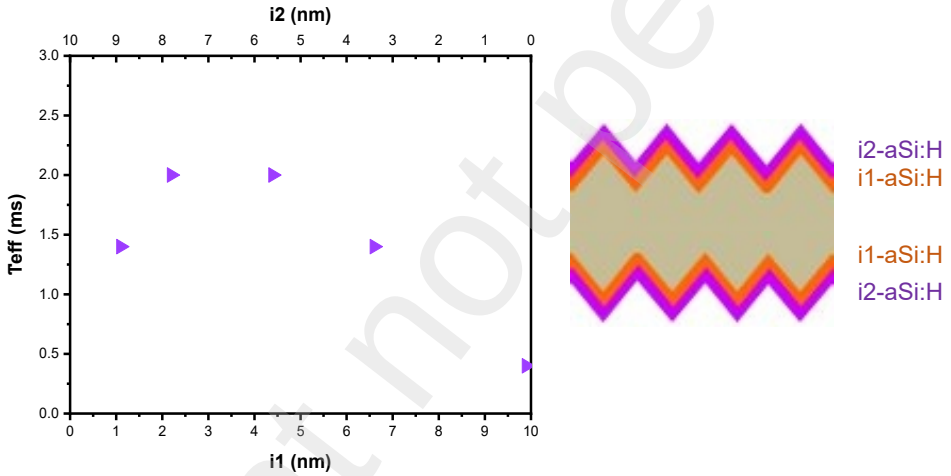

Fig. 5. Effect of the i1- to i2-layer thickness ratio on the effective lifetime (@ MCD = 10^{15} cm^{-3}) of passivated wafers with i2/i1/N/ i1/ i2 structures. The total thickness of the intrinsic bilayers is fixed at 10 nm.

We repeated a similar experiment to ensure the reliability of our results. Four low resistivity, textured wafers which went thorough same processes, were positioned in different locations on the PECVD holder (Figure 6). Two of these wafers were divided into four pieces (B and C) each to be used in a different run, while the other two remained as full wafers (A and D). For each deposition run, during which the thickness of the first layer of i-aSi:H stacks was varied, the wafers were replaced with the new ones.

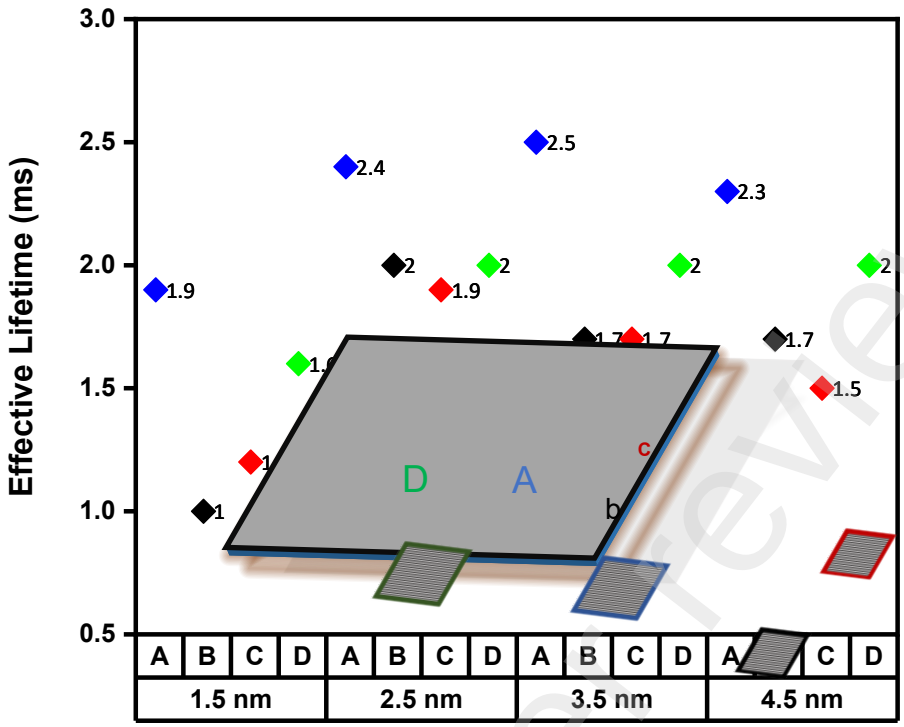

Fig. 6. Effect of the i1-layer thickness on the effective lifetime of passivated wafers with i2/i1/N/ i1/ i2 structures. The total thickness of the intrinsic bilayers is fixed at 10 nm. Post HPT time was 34 sec.

As the thickness of the first layer increased from 1.5 nm to 2.5 nm, an increase in lifetime value, measured from all wafers, was observed. However, it was also found that the position of the wafer on the holder influenced passivation. Specifically, the wafer placed at the center(A) exhibited the highest passivation, likely due to being coated with superior quality.

3.3 Impact of First Layer Porosity on Carrier Lifetimes

Porosity of first(i1) layer of intrinsic i:a-Si:H bi-layers(i1/i2) was varied by plasma power or SiH_4/H_2 flow ratio and we investigated its effect on minority carrier lifetime.

A slight peak shift is observed for the absorption of high-stretching modes around 2100 cm^{-1} (due to dihydrides, SiH_2[15]) to lower wavenumber when power decreased to 200 W (80 mW cm^{-2}) from 300 W (120 mW cm^{-2}) for 25 nm of i:a-Si films deposition, silane flow ratio (SiH_4:H_2) was 640 sccm:160 sccm. A more substantial variation was observed in the intensities of HSM and LSM than in the shift alone. Specifically, HSM intensity increased, whereas LSM intensity decreased. As a result, the films deposited at 200 W presented the highest R* (Figure 7), indicating highest porosity and highest H content.

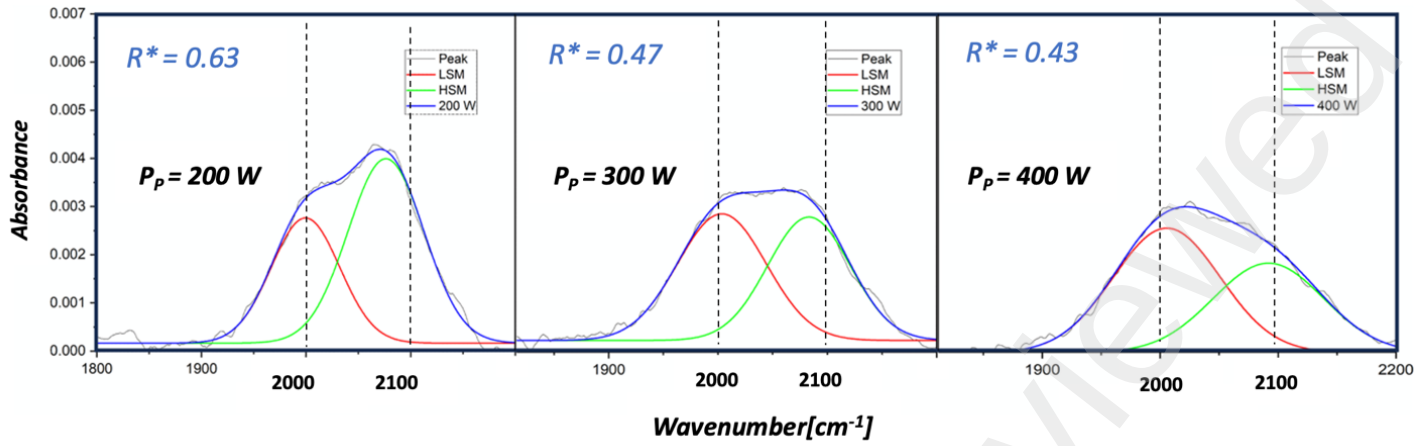

Fig. 7. FTIR spectra for i-a-Si:H layers deposited at different process powers, fitted with two Gaussian-distributed absorption peaks centered at wavenumbers of 2000 cm^{-1} and 2100 cm^{-1}, representing low (Si-H bond) and high (Si-H_2 bond) stretching modes, respectively.

Similarly, porosity can be controlled with the variation of hydrogen dilution[20]. High dilution etches the layer and avoiding void formation during a-Si:H growth thus resulting in a layer with increased density[21]. Decreasing the SiH_4/H_2 flow ratio to 1:2 from 1:4 for 25 nm i:a-Si film depositions, significantly increased the R* from 0.47 to 0.78 (Figure 8), while process power 300 W. The layer deposited by SiH_4:H_2= 1:2 has the highest R* (Figure 9), indicating highest porosity and highest H content.

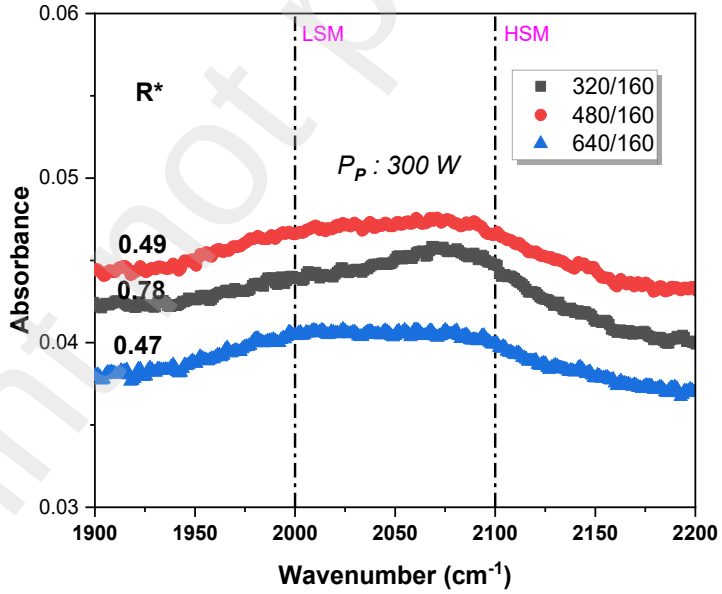

Fig. 8. Microstructure factor (R*) and absorbance spectra of the 25 nm a-Si:H films grown at 300 W using different SiH_4:H_2 flow ratios for the plasma.

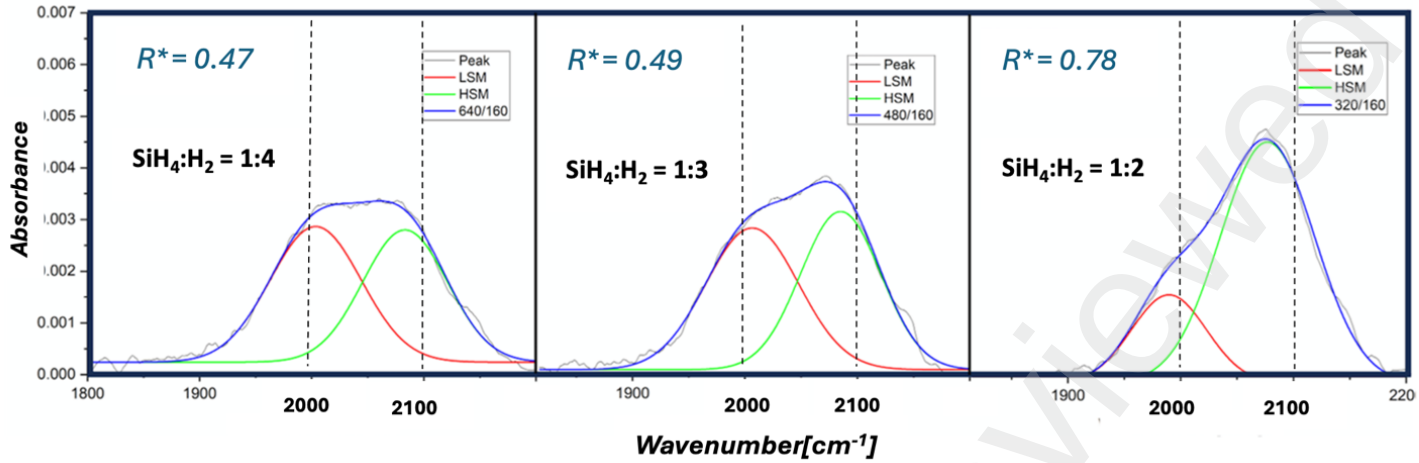

Fig. 9. FTIR spectra for i-a-Si:H layers deposited at 300 W using different SiH_4:H_2 flow ratios, fitted with two Gaussian-distributed absorption peaks centered at wavenumbers of 2000 cm^{-1} and 2100 cm^{-1}, representing low (Si-H bond) and high (Si-H_2 bond) stretching modes, respectively.

Figure 10 shows how the minority carrier lifetime changes for bilayers depending on the microstructure factors of the first layers we obtained by changing the process power or plasma dilution. Using 200 W instead of 300 W, for the first layer (3.5 nm) of 10 nm thin film deposition did not increase surface passivation further. Although total H content increase (in the form of poly-hydrides) when we change deposition power from 300 W to 200 W (Figure 7), H atoms in the form of Si–H bonds were preferred than those in the form of Si–H_2 bonds to terminate dangling bonds on the c-Si surface. Because layers deposited using SiH_4:H_2= 1:4 better Si-H bonds, using SiH_4:H_2= 1:2 for the first layer deposition did not increase surface passivation too.

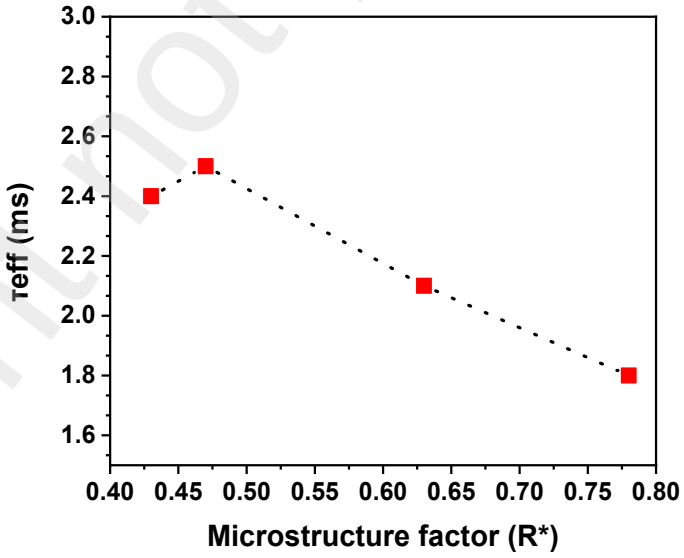

Fig. 10. Lifetime at MCD 10^{15} cm^{-3} of the passivated wafers with i2/i1/N/i/i2 structures where i1=3.5 nm and i2=6.5 nm, as a function of the microstructure factor R* of the i1-layers.

3.4 Impact of Hydrogen Plasma Treatment

Finally, these bilayers are subjected to hydrogen plasma treatment (HPT). Hydrogen plasma treatment, like hydrogen dilution of SiH_4 plasma, is a process condition might modify microstructural characteristics and affects defect density[8,22–25],[26] which is closely related to surface passivation. The HPTs incorporate additional H into the films and increase passivation[27]. However, deterioration of the passivation is also possible when the exposure time exceeds an optimal value[28,29].Therefore the HPT duration must be re-optimized for each newly introduced layer. The absorption from the vibrational states shows that the micro-structure factor of 25 nm layers (R*) deposited at 50 W or 300 W did not change significantly with HPT (Figure 11). However, the overall H content in the layers improves (the total area under the SiH and SiH_2 peaks is larger in FTIR spectra) and an increase in bandgap with HPT is observed for the 10 nm film (Figure 2).

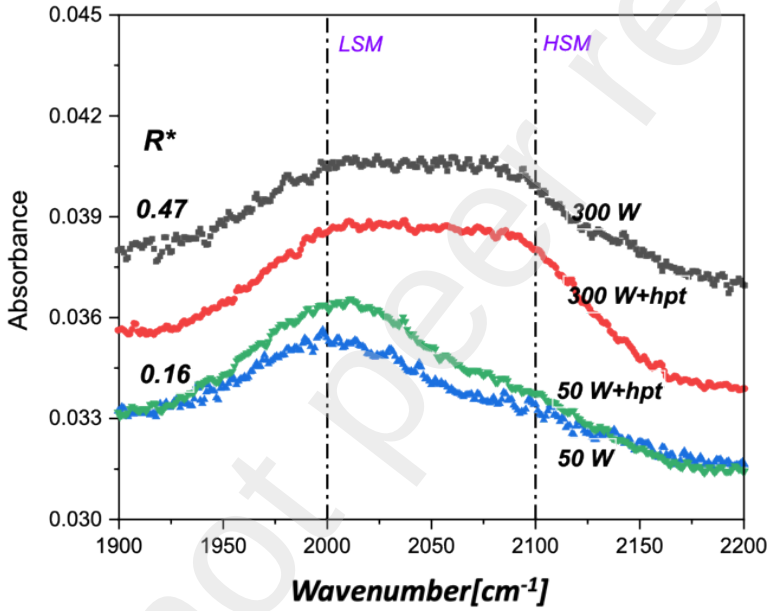

Fig. 11. Microstructure factor (R*) and absorbance spectra of the 25 nm a-Si:H films grown at 300 W or 50W before and after HPT.

We try to find an optimum condition of HPT by tuning the amount of H* species in the chamber by HPT time. HPT was applied at 50 W, after i-aSi:H bilayer depositions, for 34 s or 51 s. We can observe that increasing the post HPT time is more effective when the first porous layer of bilayer structure is very thin (1.5 nm) (Figure 12a). We investigated the effective lifetime values by systematically varying the thickness of the first layer and/or the HPT time across different days. Our findings confirmed the existence of a correlation between these parameters (Figure 12b).

When degree of disorder of the film increased, diffusion energy of atomic H can be increased (by a reduced Si-Si reconstruction energy or by the influence of isolated dangling bonds acting as traps) [30], it becomes more difficult for hydrogen to migrate within the a-Si layer. On the other hand, in dense a-Si:H, solubility limits only thermal hydrogen diffusion (like annealing related) within the dense material but atomic hydrogen in-diffusion from outside by H plasma is not affected [5]. Consequently, the porous layer is the limiting layer for H diffusion coming from HPT for our bilayer structures. Hydrogen atoms may struggle to reach the dangling bonds at the c-Si/a-Si interface when first porous layer is thicker,

reducing the effectiveness of passivation. The optimum HPT time may be longer for bilayers having thicker first layer.

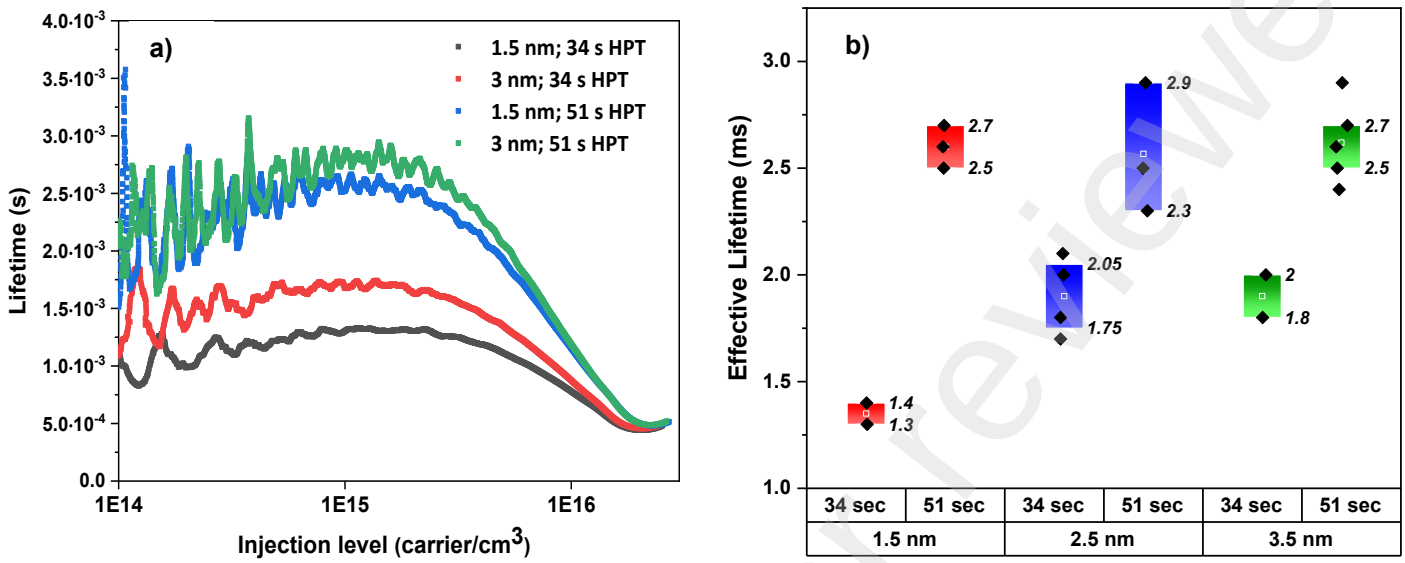

Fig. 12. a) QSSPC measurements b) Lifetime at minority carrier density 10^{15} cm^{-3} for 10 nm bilayers having different i1 thickness and treated with H_2 plasma for 34s or 51s.

4. Conclusions

This work emphasizes the critical role of intrinsic amorphous silicon (i-aSi) bilayers, which comprise both a porous and a dense layer, in enhancing passivation at the c-Si/i-aSi interface. Bilayers are optimized by systematically varying the deposition parameters. The experiments showed that the hydrogen dilution ratio and deposition power density influence the porosity of i-a-Si:H layers. Structural properties (layer porosity and hydrogen content) of the layers are correlated with minority carrier lifetime. The passivation at the c-Si and i-aSi interface can be improved by adjusting the thickness(~3nm) and microstructure factor(~0.5) of the first layer in the bilayer structure. Although our results suggest that passivation directly dependent on the Si-H concentration of interfacial layer, only the power density and hydrogen dilution of SiH_4 plasma were varied in this study. It is necessary to verify whether the same correlation persists by altering other growth parameters, such as temperature and pressure. Furthermore, this study demonstrates the relationship between passivation quality of bilayers and post hydrogen plasma treatment (HPT) time. When first layer is thinner, a more rapid increase in minority carrier lifetime value is observed by extension of post-HPT time. We explained this result with the diffusivity of atomistic hydrogen through the porous layer. These findings contribute to ongoing advancements in passivation and offer insights for further development of high-efficiency SHJ solar cells. Bilayers must also be studied as transport channels to fully evaluate their impact on overall device efficiency. Surface passivation at the a-Si: H/c-Si interface is strongly affected also by overlying doped layers[31], especially the p-layer deposition[32], and the subsequent deposition of the transparent conductive oxide. For the next step, the passivation quality of bilayers will be checked after the doped layers deposition. SHJ solar cells will be fabricated using the developed i-aSi:H bilayers and their performances will be investigated.

Acknowledgement

This work is supported by the Scientific and Technological Research Council of Turkey (TUBITAK) under grant number 20AG002 .
The authors thank A. Salimi from ODTU GUNAM for her support in fitting the ATR spectra presented by Gaussian function.

REFERENCES

[1] H. Lin, M. Yang, X. Ru, G. Wang, S. Yin, F. Peng, C. Hong, M. Qu, J. Lu, L. Fang, C. Han, P. Procel, O. Isabella, P. Gao, Z. Li, X. Xu, Silicon heterojunction solar cells with up to 26.81% efficiency achieved by electrically optimized nanocrystalline-silicon hole contact layers, Nat Energy 8 (2023) 789–799. https://doi.org/10.1038/s41560-023-01255-2.

[2] S. De Wolf, S. Olibet, C. Ballif, Stretched-exponential a-Si:Hc-Si interface recombination decay, Appl Phys Lett 93 (2008). https://doi.org/10.1063/1.2956668.

[3] S.K. Kim, J.C. Lee, S.J. Park, Y.J. Kim, K.H. Yoon, Effect of hydrogen dilution on intrinsic a-Si:H layer between emitter and Si wafer in silicon heterojunction solar cell, Solar Energy Materials and Solar Cells 92 (2008) 298–301. https://doi.org/10.1016/j.solmat.2007.09.007.

[4] X. Qu, Y. He, M. Qu, T. Ruan, F. Chu, Z. Zheng, Y. Ma, Y. Chen, X. Ru, X. Xu, H. Yan, L. Wang, Y. Zhang, X. Hao, Z. Hameiri, Z.G. Chen, L. Wang, K. Zheng, Identification of embedded nanotwins at c-Si/a-Si:H interface limiting the performance of high-efficiency silicon heterojunction solar cells, Nat Energy 6 (2021) 194–202. https://doi.org/10.1038/s41560-020-00768-4.

[5] H. Sai, H.J. Hsu, P.W. Chen, P.L. Chen, T. Matsui, Intrinsic Amorphous Silicon Bilayers for Effective Surface Passivation in Silicon Heterojunction Solar Cells: A Comparative Study of Interfacial Layers, Physica Status Solidi (A) Applications and Materials Science 218 (2021). https://doi.org/10.1002/pssa.202000743.

[6] H. Sai, P.W. Chen, H.J. Hsu, T. Matsui, S. Nunomura, K. Matsubara, Impact of intrinsic amorphous silicon bilayers in silicon heterojunction solar cells, J Appl Phys 124 (2018). https://doi.org/10.1063/1.5045155.

[7] B. Fischer, W. Beyer, A. Lambertz, M. Nuys, W. Duan, K. Ding, U. Rau, The Microstructure of Underdense Hydrogenated Amorphous Silicon and its Application to Silicon Heterojunction Solar Cells, Solar RRL 7 (2023). https://doi.org/10.1002/solr.202300103.

[8] Y. Zhao, P. Procel, A. Smets, L. Mazzarella, C. Han, G. Yang, L. Cao, Z. Yao, A. Weeber, M. Zeman, O. Isabella, Effects of (i)a-Si:H deposition temperature on high-efficiency silicon heterojunction solar cells, Progress in Photovoltaics: Research and Applications 31 (2023) 1170–1180. https://doi.org/10.1002/pip.3620.

[9] H. Meddeb, T. Bearda, Y. Abdelraheem, H. Ezzaouia, I. Gordon, J. Szlufcik, J. Poortmans, Structural, hydrogen bonding and in situ studies of the effect of hydrogen dilution on the passivation by amorphous silicon of n-type crystalline (1 0 0) silicon surfaces, J Phys D Appl Phys 48 (2015). https://doi.org/10.1088/0022-3727/48/41/415301.

[10] K.S. Lee, C.B. Yeon, S.J. Yun, K.H. Jung, J.W. Lima, Improved surface passivation using dual-Layered a-Si:H for silicon heterojunction solar cells, ECS Solid State Letters 3 (2014). https://doi.org/10.1149/2.001404ssl.

[11] A.H.M. Smets, W.M.M. Kessels, M.C.M. Van de Sanden, Vacancies and voids in hydrogenated amorphous silicon, Appl Phys Lett 82 (2003) 1547–1549. https://doi.org/10.1063/1.1559657.

[12] A.A. Langford, M.L. Fleet, B.P. Nelson, W.A. Lanford, N. Maley, Infrared absorption strength and hydrogen content of hydrogenated amorphous silicon, n.d.

[13] X. Ru, M. Qu, J. Wang, T. Ruan, M. Yang, F. Peng, W. Long, K. Zheng, H. Yan, X. Xu, 25.11% efficiency silicon heterojunction solar cell with low deposition rate intrinsic amorphous silicon buffer layers, Solar Energy Materials and Solar Cells 215 (2020). https://doi.org/10.1016/j.solmat.2020.110643.
[14] B. Fischer, A. Lambertz, M. Nuys, W. Beyer, W. Duan, K. Bittkau, K. Ding, U. Rau, Insights into the Si─H Bonding Configuration at the Amorphous/Crystalline Silicon Interface of Silicon Heterojunction Solar Cells by Raman and FTIR Spectroscopy, Advanced Materials 35 (2023). https://doi.org/10.1002/adma.202306351.
[15] H. Fujiwara, Y. Toyoshima, M. Kondo, A. Matsuda, Interface-layer formation mechanism in a-Si:H thin-film growth studied by real-time spectroscopic ellipsometry and infrared spectroscopy, n.d.
[16] A. Canillas, E. Bertran, J.L. Andújar, B. Drévillon, In situ spectroellipsometric study of the nucleation and growth of amorphous silicon, J Appl Phys 68 (1990) 2752–2759. https://doi.org/10.1063/1.346452.
[17] S. Kim, V.A. Dao, C. Shin, J. Cho, Y. Lee, N. Balaji, S. Ahn, Y. Kim, J. Yi, Low defect interface study of intrinsic layer for c-Si surface passivation in a-Si:H/c-Si heterojunction solar cells, in: Thin Solid Films, 2012: pp. 45–49. https://doi.org/10.1016/j.tsf.2012.03.074.
[18] L. Zhao, H. Diao, X. Zeng, C. Zhou, H. Li, W. Wang, Comparative study of the surface passivation on crystalline silicon by silicon thin films with different structures, Physica B Condens Matter 405 (2010) 61–64. https://doi.org/10.1016/j.physb.2009.08.024.
[19] J. Ge, Z.P. Ling, J. Wong, T. Mueller, A.G. Aberle, Optimisation of intrinsic a-Si:H passivation layers in crystalline- amorphous silicon heterojunction solar cells, in: Energy Procedia, 2012: pp. 107–117. https://doi.org/10.1016/j.egypro.2012.02.013.
[20] K.S. Lee, C.B. Yeon, S.J. Yun, K.H. Jung, J.W. Lima, Improved surface passivation using dual-Layered a-Si:H for silicon heterojunction solar cells, ECS Solid State Letters 3 (2014). https://doi.org/10.1149/2.001404ssl.
[21] D. Deligiannis, R. Vasudevan, A.H.M. Smets, R.A.C.M.M. van Swaaij, M. Zeman, Surface passivation of c-Si for silicon heterojunction solar cells using high-pressure hydrogen diluted plasmas, AIP Adv 5 (2015). https://doi.org/10.1063/1.4931821.
[22] L. Zhang, W. Guo, W. Liu, J. Bao, J. Liu, J. Shi, F. Meng, Z. Liu, Investigation of positive roles of hydrogen plasma treatment for interface passivation based on silicon heterojunction solar cells, J Phys D Appl Phys 49 (2016). https://doi.org/10.1088/0022-3727/49/16/165305.
[23] A. Soman, U. Nsofor, U. Das, T. Gu, S. Hegedus, Correlation between in Situ Diagnostics of the Hydrogen Plasma and the Interface Passivation Quality of Hydrogen Plasma Post-Treated a-Si:H in Silicon Heterojunction Solar Cells, ACS Appl Mater Interfaces 11 (2019) 16181–16190. https://doi.org/10.1021/acsami.9b01686.
[24] A. Neumüller, O. Sergeev, S.J. Heise, S. Bereznev, O. Volobujeva, J.F.L. Salas, M. Vehse, C. Agert, Improved amorphous silicon passivation layer for heterojunction solar cells with post-deposition plasma treatment, Nano Energy 43 (2018) 228–235. https://doi.org/10.1016/j.nanoen.2017.11.053.
[25] S.M. Karabanov, M. Reginevich, Impact of Hydrogen Plasma Treatment on Intrinsic Amorphous Silicon Bilayers in Silicon Heterojunction Solar Cells, in: 21st IEEE International Conference on Environment and Electrical Engineering and 2021 5th IEEE Industrial and Commercial Power System Europe, EEEIC / I and CPS Europe 2021 - Proceedings, Institute of Electrical and Electronics Engineers Inc., 2021. https://doi.org/10.1109/EEEIC/ICPSEurope51590.2021.9584467.
[26] W. Liu, L. Zhang, R. Chen, F. Meng, W. Guo, J. Bao, Z. Liu, Underdense a-Si:H film capped by a dense film as the passivation layer of a silicon heterojunction solar cell, J Appl Phys 120 (2016). https://doi.org/10.1063/1.4966941.
[27] Y. Zhang, C. Yu, M. Yang, L.R. Zhang, Y.C. He, J.Y. Zhang, X.X. Xu, Y.Z. Zhang, X.M. Song, H. Yan, Significant Improvement of Passivation Performance by Two-Step Preparation of Amorphous Silicon Passivation Layers in Silicon Heterojunction Solar Cells, Chinese Physics Letters 34 (2017). https://doi.org/10.1088/0256-307X/34/3/038101.

[28] S.N. Granata, T. Bearda, F. Dross, I. Gordon, J. Poortmans, R. Mertens, Effect of an in-situ H2 plasma pretreatment on the minority carrier lifetime of a-Si:H(i) passivated crystalline silicon, in: Energy Procedia, Elsevier Ltd, 2012: pp. 412–418. https://doi.org/10.1016/j.egypro.2012.07.086.
[29] A. Descoeudres, L. Barraud, S. De Wolf, B. Strahm, D. Lachenal, C. Guérin, Z.C. Holman, F. Zicarelli, B. Demaurex, J. Seif, J. Holovsky, C. Ballif, Improved amorphous/crystalline silicon interface passivation by hydrogen plasma treatment, Appl Phys Lett 99 (2011). https://doi.org/10.1063/1.3641899.
[30] W. Beyer, H. Wagner, Determination of the hydrogen diffusion coefficient in hydrogenated amorphous silicon from hydrogen effusion experiments, J Appl Phys 53 (1982) 8745–8750. https://doi.org/10.1063/1.330474.
[31] Z. Wu, L. Zhang, R. Chen, W. Liu, Z. Li, F. Meng, Z. Liu, Improved amorphous/crystalline silicon interface passivation for silicon heterojunction solar cells by hot-wire atomic hydrogen during doped a-Si:H deposition, Appl Surf Sci 475 (2019) 504–509. https://doi.org/10.1016/j.apsusc.2018.12.239.
[32] H. Sai, H. Umishio, T. Matsui, S. Nunomura, T. Kawatsu, H. Takato, K. Matsubara, Impact of silicon wafer thickness on photovoltaic performance of crystalline silicon heterojunction solar cells, in: Jpn J Appl Phys, Japan Society of Applied Physics, 2018. https://doi.org/10.7567/JJAP.57.08RB10.